Lown, J. W. (1977) *Biorg. Chem. 3*, 95–121.
Muller, W., & Crothers, D. M. (1968) *J. Mol. Biol. 35*, 251–290.
Pardi, A., Walker, R., Rapoport, H., Wider, G., & Wüthrich, K. (1983) *J. Am. Chem. Soc. 105*, 1652.
Patel, D. J. (1974) *Biochemistry 13*, 2396.
Patel, D. J. (1976) *Biopolymers 15*, 533.
Patel, D. J. (1979a) *Acc. Chem. Res. 12*, 118.
Patel, D. J. (1979b) in *Stereodynamics of Molecular Systems*, pp 397–472, Pergamon Press, New York.
Patel, D. J. (1979c) *Eur. J. Biochem. 96*, 267.
Patel, D. J. (1979d) *Eur. J. Biochem. 99*, 369.
Patel, D. J., Kozlowski, S. A., Rice, J. A., Broka, C., & Itakura, K. (1981) *Proc. Natl. Acad. Sci. U.S.A. 78*, 7281–7284.
Petersheim, M., Mehdi, S., & Gerlt, J. A. (1984) *J. Am. Chem. Soc. 106*, 439.
Pople, J. A., Schneider, W. G., & Bernstein, H. J. (1959) *High Resolution Nuclear Magnetic Resonance*, Chapters 9 and 10, McGraw-Hill, New York.
Prado, F. R., Giessner-Prettre, C., Pullman, B., & Daudey, J.-P. (1979) *J. Am. Chem. Soc. 101*, 1737–1742.
Reddy, B. S., Seshadri, T. P., Sakore, T. D., & Sobell, H. M. (1979) *J. Mol. Biol. 135*, 787.
Reid, D. G., Salisbury, S. A., & Williams, D. H. (1983) *Biochemistry 22*, 1377–1385.
Reinhardt, C. G., & Krugh, T. R. (1977) *Biochemistry 16*, 2890.
Remers, W. A. (1978) in *The Chemistry of Antitumor Antibiotics*, Vol. 1, Wiley, New York.
Sarma, R. H., Dhingra, M. (1981) M. in *Topics in Nucleic Acid Structure* (Neidle, S., Ed.) Chapter 3, Wiley, New York.
Scheek, R. M., Russo, N., Boelens, R., Kaptein, R., & Van Boom, J. H. (1983) *J. Am. Chem. Soc. 105*, 2914–2916.
Seela, F., Ott, J., & Potter, B. V. C. (1983) *J. Am. Chem. Soc. 105*, 5879.
Shieh, H.-S., Berman, H. M., Debrow, M., & Neidle, S. (1980) *Nucleic Acids Res. 8*, 85.
Stec, W. J. (1983) *Acc. Chem. Res. 16*, 411.
Takusagawa, F., Dabrow, M., Neidle, S., & Berman, H. M. (1982) *Nature (London) 296*, 466–469.
Tanaka, T., & Letsinger, R. L. (1982) *Nucleic Acids Res. 10*, 3249.
Tsai, M. D. (1984) in *^{31}P NMR: Principles and Applications* (Gorenstein, D. G., Ed.) Chapter 6, Academic Press, New York.
Ts'o, P. O. P. (1975) *Basic Principles in Nucleic Acid Chemistry*, Vol. I and II, Academic Press, New York and London.

$2NH_2A{\cdot}T$ Helices in the Ribo- and Deoxypolynucleotide Series. Structural and Energetic Consequences of $2NH_2A$ Substitution†

Frank B. Howard* and H. Todd Miles*

ABSTRACT: Polynucleotide helices formed by the interaction of $(d2NH_2A)_n$, $(r2NH_2A)_n$, $(dT)_n$, and $(rT)_n$ have been prepared and their physical and spectroscopic properties examined. Thermal transitions, dependence of T_m on salt concentration, stoichiometry, phase diagrams, and calculated enthalpies are reported. UV, CD, and IR spectra are reported. All of the deoxy–deoxy helices containing $2NH_2A$ have positive CD first extrema near 290 nm and appear to have B-form structure. All the ribo–ribo or hybrid helices have negative first extrema in this region and appear to have A-form structure. Elevation of T_m by the 2-NH_2 group of $2NH_2A$ is much smaller in the deoxy than in the ribo series. We have applied an equation based on the electrostatic theory of Manning [Manning, G. S. (1972) *Bopolymers 11*, 937–949; Manning, G. S. (1978) *Q. Rev. Biophys. 11*, 179–246; Record, M. T., Anderson, C. F., & Lohman, T. M. (1978) *Q. Rev. Biophys. 11*, 103–178] to calculate ethalpies of the helix–coil transitions of the complexes reported here. These calculated enthalpies are larger for $2NH_2A{\cdot}T$ than for $A{\cdot}T$ helices, but the difference is much smaller in the deoxy than in the ribo series. We attribute these effects on T_m and ΔH in the deoxy series to loss of stabilization of the spine of hydration in B-form structures caused by interference of the 2-NH_2 group in the minor groove of the helix [Dickerson, R. E., Drew, H. R., Conner, B. N., Wing, R. M., Fratini, A. V., & Kopka, M. L. (1982) *Science (Washington, D.C.) 216*, 475–485]. Complete phase diagrams for all $2NH_2A$,T systems and some A,T systems are reported. The diagrams differ widely and can be placed in four groups according to the number of transitions each system possesses.

Introduction of a 2-NH_2 group into adenine residues of polynucleotides significantly perturbs their physical and spectroscopic properties, while maintaining base pairing specificity to uracil and thymine. A major chemical change occurs in the formation of three rather than two hydrogen bonds in AT and AU base pairs. These changes have been examined in detail in the ribopolynucleotide series (Howard et al., 1966, 1976; Muraoka et al., 1980). Preliminary studies in the deoxy series (Howard & Miles, 1983a,b; Howard et al., 1984) have shown striking contrasts from the ribo series in transition temperatures and circular dichroism (CD). In this paper we examine homopolymer systems containing $2NH_2A$ and T residues in the ribo and deoxy series with emphasis on the differences between the two. Relevance of the new data to the familiar three H-bond GC pair is also examined by using available data from the literature. The high transition temperatures of GC helices and the very stable self-structure of poly(G) have hindered or prevented direct observation of many

† From the Laboratory of Molecular Biology, National Institute of Arthritis, Diabetes, and Digestive and Kidney Diseases, National Institutes of Health, Bethesda, Maryland 20205. *Received June 21, 1984.*

thermal properties of actual or potential complexes of G. Insight into some of these properties may be obtained, however, by observation of $2NH_2A$ polymers in accessible temperature ranges.

Materials and Methods

The procedure for determining mixing curves has been described (Howard et al., 1971, 1976). A separate solution was prepared for each composition. UV spectra were measured with a Cary Model 118 spectrophotometer interfaced to an LDACS computer system (Powell et al., 1980). Use of a computer to analyze the data has been described (Howard et al., 1976).

Melting curves were measured automatically, the Cary 118 spectrophotometer and accessory equipment operating in a closed-loop mode with the LDACS system (Howard et al., 1977).

CD spectra were recorded with a Jasco J-500A spectropolarimeter also connected to the LDACS system.

2-Aminodeoxyadenosine (lot no. 874001), $p(dA)_7$ (lot no. 637-83), $p(dC)_6$ (lot no. 68452), and poly(dT) (lot no. 668/105) were from P-L Biochemicals. Synthesis of poly(rT) has been described (Howard et al., 1971).

Synthesis of 2-Aminodeoxyadenosine 5'-Phosphate. 2-Aminodeoxyadenosine is extremely labile in acid, and attempts to synthesize the monophosphate by phosphorylation with $POCl_3$ (Yoshikawa et al., 1969) at $[POCl_3]/[\text{nucleoside}]$ ratios of 1.25, 2.00, or 3.06 at −14 °C resulted in yields of <10%. Although synthesis of 2-aminodeoxyadenosine 5'-phosphate by the method of Tener (1961) has been reported (Cerami et al., 1967), we find that pyridinium ion formed in the preparation of 2-cyanoethyl phosphate is sufficiently acidic to catalyze a rapid and complete depurination of 2-aminodeoxyadenosine. Addition of sufficient triethylamine to neutralize pyridinium ion, however, prevents any loss of the starting nucleoside and allows phosphorylation to proceed.

To a solution of 2-aminodeoxyadenosine (0.300 g, 1.128 mmol) in 15 mL of 50% aqueous pyridine was added 5.40 mL of a solution containing 4.22 mmol of 2-cyanoethyl phosphate and 8.44 mmol of triethylamine in pyridine. The mixture was evaporated to dryness in vacuo (bath <30 °C) and rendered anhydrous by three evaporations of 15 mL of dry pyridine. The residue was dissolved in 30 mL of dry pyridine, and 2.950 g (14.30 mmol) of dicyclohexylcarbodiimide (DCC) was added. The reaction mixture was stored in the dark at 25 °C. An additional 2.246 g (10.89 mmol) of DCC was added after 20 h. After 3 days, the reaction was stopped with 1 mL of water. The mixture was stirred for 10 min and concentrated to dryness in vacuo. The residue was suspended in 30 mL of 0.4 M lithium hydroxide and heated under reflux for 1 h. The cooled mixture was filtered and the solid washed 3 times with 2 mL volumes of water.

The filtrate (pH 10.7) was applied to a 2.5 × 26 cm column of DEAE-Sephadex (Bicarbonate form). Neutral material was removed with a water wash (1190 mL), and the column was developed with a linear gradient consisting of 1 L of water in the mixing bottle and 1 L of 0.2 M triethylammonium bicarbonate in the reservoir. 2-Aminodeoxyadenosine 5'-phosphate appeared in tubes 160–199 (704 mL; flow rate 2.56 mL/min). Pooled fractions were concentrated to dryness in vacuo and water evaporated several times to remove residual triethylammonium bicarbonate. The product was recovered in 8.59 mL of water. Yield, based on UV measurements, was 0.614 mmol (54.7%).

Analysis showed that 2-aminodeoxyadenosine 5'-phosphate was contaminated with 9.4% inorganic phosphate. A second cycle of ion-exchange chromatography, however, reduced the inorganic phosphate content to 0.2%.

The molar extinction coefficient was determined by analysis for phosphorus as described previously (Muraoka et al., 1980). The mean of four determinations was 9630 (279 nm) with a standard deviation of 180.

Progress of the phosphorylation was monitored by thin-layer chromatography. At intervals, 20 μL of the reaction mixture was transferred to 40 μL of 0.4 M lithium hydroxide and heated in a boiling water bath for 1 h. Samples were applied to a cellulose thin-layer sheet (J. T. Baker Chemical Co.), and the chromatogram was developed in 1-propanol-concentrated ammonium hydroxide–water (60:30:10) for 4.5 h: 2-aminodeoxyadenosine, R_f 0.63; 2-aminodeoxyadenosine 5'-phosphate, R_f 0.20; 2,6-diaminopurine, R_f 0.45.

Thin-layer chromatography of a venom (*Crotalus adamanteus*) digest of 2-aminodeoxyadenosine 5'-phosphate with the above solvent system showed a single blue fluorescent spot (under UV illumination) with the same R_f as authentic 2-aminodeoxyadenosine.

Synthesis of 2-Aminodeoxyadenosine 5'-Phosphomorpholidate. We synthesized 2-aminodeoxyadenosine 5'-phosphomorpholidate in 80.5% yield by following the general procedure of Moffatt & Khorana (1961). ε(279 nm) = 10600 ± 220 (four determinations).

Synthesis of 2-Aminodeoxyadenosine 5'-Triphosphate. 2-Aminodeoxyadenosine 5'-triphosphate was synthesized from bis(tri-*n*-butylammonium) pyrophosphate and 2-aminodeoxyadenosine 5'-phosphomopholidate by the procedure of Moffatt & Khorana (1961) with the substitution of dimethylformamide for pyridine as the solvent. Yield of triphosphate from 8.25×10^{-2} mmol of 2-aminodeoxyadenosine 5'-phosphomorpholidate was 5.42×10^{-2} mmol (70.8%). ε(279 nm) = 9240 ± 190 (four determinations).

The triphosphate was submitted to cellulose thin-layer electrophoresis in 0.05 M citrate, pH 5.0, at 150 V, 8 mA, for 4 h. The following are migration rates (relative to 2-aminodeoxyadenosine 5'-phosphate): 2 aminodeoxyadenosine 5'-triphosphate, 5.27; deoxyadenosine 5'-phosphate, 2.38; adenosine 5'-diphosphate, 4.88; deoxyadenosine 5'-triphosphate, 5.80; 2-aminodeoxyadenosine 5'-phosphomorpholidate, 0.88. No other UV-absorbing component was detected in the desired triphosphate.

Thin-layer chromatography of a snake venom digest of 2-aminodeoxyadenosine 5'-triphosphate with the solvent system described above resulted in a single blue fluorescent spot with the same R_f as authentic 2-aminodeoxyadenosine and no other UV-absorbing compounds.

The triphosphate was analyzed for inorganic pyrophosphate by incubating samples with inorganic pyrophosphatase and measuring inorganic phosphate in the hydrolysate. The level of contamination was found to be 3.2%.

Synthesis of Poly($d2NH_2A$). An 8-mL reaction mixture contained the following components: 2×10^{-3} M 2-aminodeoxyadenosine 5'-triphosphate; 5.95×10^{-5} M $p(dA)_7$, 0.04 M potassium cacodylate, pH 7.5; 8×10^{-3} M magnesium chloride; 5.53×10^{-4} M zinc sulfate; 0.8 mL of E730 diluent (Willis et al., 1980); 2400 units of terminal deoxynucleotidyltransferase from calf thymus (Bollum, 1966; Willis et al., 1980). Progress of the reaction in a 0.3-mL aliquot was followed by the decrease in absorbance at 278 nm observed on the monitor of an LDACS–spectrophotometer system (1-mm path length; 37 °C), while the remainder of the reaction mixture was incubated separately at 37 °C. After 27.6 h, 0.06 mL of concentrated ammonium hydroxide was added and the

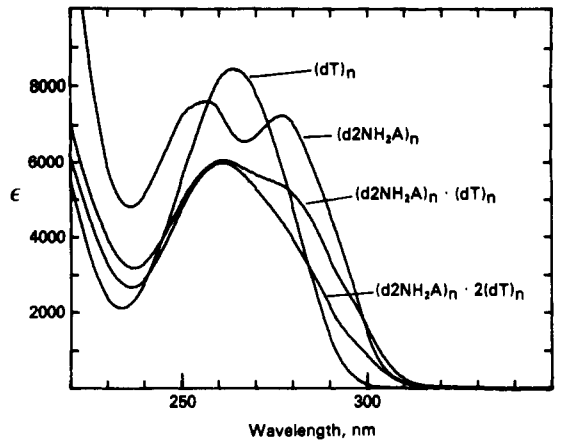

FIGURE 1: Ultraviolet spectra at 4.8 °C of poly(d2NH$_2$A), poly(d2NH$_2$A)·poly(dT), poly(d2NH$_2$A)·2poly(dT), and poly(dT). Conditions: 8 × 10^{-5} M total polymer P, 0.002 M sodium pyrophosphate, pH 8.0; 0.1 M Na$^+$, in this and succeeding figures unless otherwise noted.

resulting white precipitate removed by centrifugation at 5000 rpm for 10 min. The supernatent twice was extracted with 5 mL of a 1:1 mixture of chloroform and phenol equilibriated with 0.1 M tris(hydroxymethyl)aminomethane (Tris) buffer, pH 8.0, and containing 0.1% 8-hydroxyquinoline (Maniatis et al., 1982). The aqueous solution was dialyzed against 2 L volumes of 1 M NaCl, 0.001 M ethylenediaminetetraacetic acid (EDTA) (24 h), 1 M NaCl (two changes, 69 h) and water (five changes, 96 h). The polymer was recovered in 8.25 mL of water and stored at −20 °C: yield 5.84 × 10^{-3} mmol (37.9%). The molar extinction coefficient was determined as described previously (Muraoka et al., 1980) with a 5-fold reduction in scale. ϵ(257 nm) = 7630 ± 70 (six determinations). The maximum possible content of (pdA)$_7$ was about 8% if we assume that all of the input oligomer was present in the isolated polymer. Electrophoresis of poly(d2NH$_2$A) end labeled with ^{32}P (Maxam & Gilbert, 1980) on a 10% polyacrylamide gel in 0.1 M Tris–borate, pH 8.3, and 2 mM EDTA for 2.5 h at 850 V indicated that more than 90% of the polymer migrated to a position delimited by markers of 234 and 1353 base pairs (ϕX174 RF DNA–*Hae*III digest, New England Biolabs).

Poly(d2NH$_2$A) was also prepared in 56% yield by substitution of p(dC)$_6$ (6.94 × 10^{-5} M) for p(dA)$_7$ as primer. Maximum content of p(dC)$_6$ was 5.6%. T_m values of complexes formed between poly(dT) or poly(rT) and p(dC)$_6$-primed poly(d2NH$_2$A) were about 1 °C higher than with the p(dA)$_7$-primed polymer.

Results

Stoichiometry. We have employed a computer-based analysis of UV spectra of mixtures of poly(d2NH$_2$A) and poly(dT) (Figure 1) to establish the combining ratios of their interaction products (cf. Howard et al., 1976, 1977; Muraoka et al., 1980). The angles θ_1 and θ_2 between the limbs of mixing curves at mole fractions X_T = 0.50 and 0.67 are computed as continuous functions of wavelength. Values of these angles (θ_1 and θ_2) are then plotted as shown in Figure 2. When $\theta \approx 180°$ over the entire wavelength range, no complex is formed at that ratio. Maxima and minima in these curves correspond to wavelengths of optimum sensitivity for detection of complexes [Table IS in the supplementary material (see paragraph at end of paper regarding supplementary material)]. Clearly both 1:1 and 1:2 complexes are formed under these conditions (Figure 3). The same ultraviolet data can also be analyzed

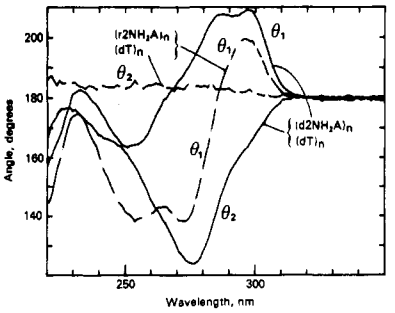

FIGURE 2: Wavelength dispersion of the angles of intersection of the mixing curves corresponding to 50% poly(dT) (θ_1) and 67% poly(dT) (θ_2) in the poly(d2NH$_2$A),poly(dT) system (solid lines) and of the mixing curves corresponding to 50% poly(dT) (θ_1) and 67% poly(dT) (θ_2) in the poly(r2NH$_2$A),poly(dT) system (broken lines). The most sensitive wavelength for detecting the 1:1 complex in the poly(d2NH$_2$A),poly(dT) system is 297 nm and for detecting the 1:2 complex, 276 nm. Favorable wavelengths for detecting the 1:1 complex in the poly(r2NH$_2$A),poly(dT) system (θ_1, broken lines) occur at 254, 272, and 296 nm. θ_2 (broken lines) is approximately 180° over the entire spectral range, indicating that a 1:2 complex is not formed. Conditions: same as those of Figure 1, except that T = 20.0 °C for the poly(r2NH$_2$A),poly(dT) system.

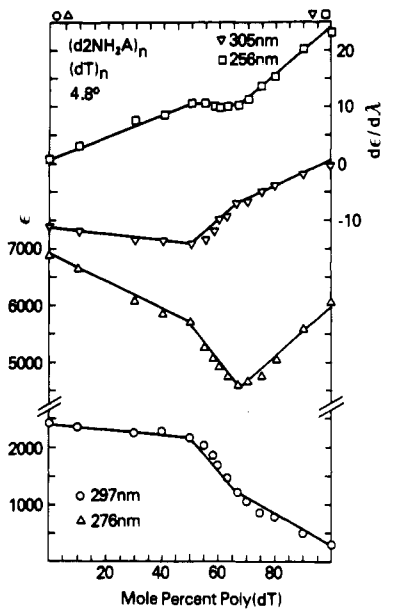

FIGURE 3: Clear breaks at 1:1 and 1:2 ratios in both ultraviolet [(o, △) left scale] and derivative ultraviolet [(▽, □) right scale] mixing curves at four different wavelengths demonstrate formation of poly(d2NH$_2$A)·poly(dT) and poly(d2NH$_2$A)·2poly(dT). T = 4.8 °C.

by generating derivative spectra (dϵ/dλ vs. λ) in the computer and plotting mixing curves from these (Howard et al., 1977), as in Figure 3. The conclusion is, of course, the same, but the sharpness of intersection is often, as here, greater than with direct absorbance plots. The optimum wavelengths, moreover, are different in the two methods, a fact that may be used to advantage in the presence of other absorbing species. CD mixing curves lead to the same conclusion (Figure 1S in supplementary material). (r2NH$_2$A)$_n$ also reacts with (rT)$_n$ to form both 1:1 and 1:2 complexes, as shown by UV mixing curves (Figure 2S in supplementary material). Mixing curves and derivative mixing curves for the interaction of (d2NH$_2$A) with (rT)$_n$ are given in Figure 4. These show that in this system also both 1:1 and 1:2 complexes are formed in 0.1 M Na$^+$ at ambient temperature, strandedness being determined by the composition of the mixture. In contrast to all of the above systems (r2NH$_2$A)$_n$ forms only a 1:1 complex with (dT)$_n$. The wavelength dispersion of the angle of intersection

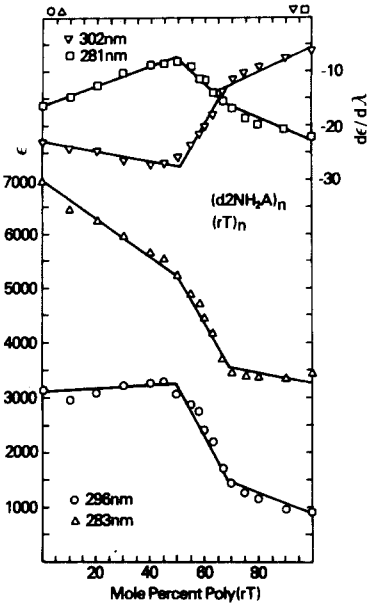

FIGURE 4: Ultraviolet [(O, △) left scale] and derivative ultraviolet [(▽, □) right scale] mixing curves at four different wavelengths demonstrate formation of poly(d2NH$_2$A)·poly(rT) and poly-(d2NH$_2$A)·poly(rT). T = 20.0 °C.

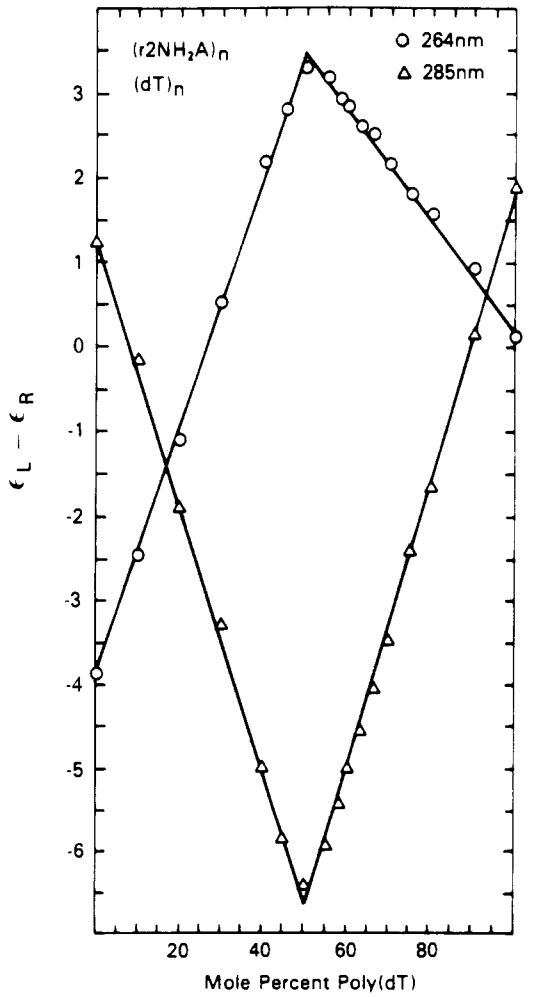

FIGURE 5: Sharp break at the 1:1 ratio in CD mixing curves (O, △) demonstrates formation of poly(r2NH$_2$A)·poly(dT). T = 20.0 °C.

shows favorable wavelengths for detecting the double helix at 254, 272, and 296 nm (Figure 2; Figure 3S in supplementary material), and $\theta_2 \simeq 180°$ at all wavelengths (Figure 2), showing that a 1:2 complex is not formed (cf. Howard et al., 1976). Confirmation of these points is obtained in the CD mixing curve, Figure 5.

Table I: Spectroscopic Data

	Ultraviolet			
	λ_{max} (nm)	ϵ_{max}	λ_{min} (nm)	ϵ_{min}
(d2NH$_2$A)$_n$[a]	257	7630	237	4900
	277	7310	267	6630
(r2NH$_2$A)$_n$[b]	256.5	7370	238	5120
	278	6580	269	6210
(d2NH$_2$A)$_n$·(dT)$_n$[a]	261	6090	237	3200
(d2NH$_2$A)$_n$·2(dT)$_n$[a]	261	6020	236	2700
(d2NH$_2$A)$_n$·(rT)$_n$[c]	263	6150	238	3220
(d2NH$_2$A)$_n$·2(rT)$_n$[c]	261	6270	239	3000
(r2NH$_2$A)$_n$·(dT)$_n$[c]	262	6120	239	3090
(r2NH$_2$A)$_n$·(rT)$_n$[c]	261	6300	239	3160
(r2NH$_2$A)$_n$·2(rT)$_n$[c]	262	6310	238	2690
	Circular Dichroism			
	λ_{max} (nm)	$\epsilon_L - \epsilon_R$	λ_{min} (nm)	$\epsilon_L - \epsilon_R$
(d2NH$_2$A)$_n$[a]	292	3.03	272	−6.59
	257	−0.71	247	−2.81
	222	23.3		
(d2NH$_2$A)$_n$·(dT)$_n$[a]	295	2.02	271	−3.41
	264	−2.88	250	−4.59
	222	11.6		
(d2NH$_2$A)$_n$·2(dT)$_n$[a]	290	0.62	249	−5.67
	226	5.99		
(d2NH$_2$A)$_n$·(rT)$_n$[c]	277	1.42	300	−2.00
	222	11.6	252	−3.28
(d2NH$_2$a)$_n$·2(rT)$_n$[c]	270	4.48	297	−1.75
	223	7.26	251	−5.14
(r2NH$_2$A)$_n$·(dT)$_n$[c]	265	3.32	284	−6.46
	221	6.03	247	−2.35
(r2NH$_2$A)$_n$·(rT)$_n$[c]	267	3.98	285	−4.60
	224	5.67	249	−2.84
(r2NH$_2$A)$_n$·2(rT)$_n$[c]	270	6.32	296	−1.89
	223	4.97	250	−4.49
(dA)$_n$·2(rT)$_n$[d]	291	0.58	267	−0.87
	256	1.51	246	−3.41
	231	0.82		
(rA)$_n$·(dT)$_n$[d]	281	2.92	247	−7.76
	259	5.33	209	−5.34
	221	1.92		
(rA)$_n$·(rT)$_n$[d]	259	7.52	246	−4.04
	225	1.54	210	−4.21
(rA)$_n$·2(rT)$_n$[d]	279	3.29	265	1.76
	257	3.21	246	−1.31
	224	1.90	210	−2.83

[a] Conditions: 0.1 M Na^+; 0.002 M sodium pyrophosphate, pH 8.1; 4.8 °C. [b] Conditions: 0.1 M Na^+; 0.005 M sodium pyrophosphate, pH 8.0; 25 °C. [c] Conditions: 0.1 M Na^+; 0.002 M sodium pyrophosphate, pH 8.0; 20.0 °C. [d] Conditions: 0.1 M Na^+; 0.002 M sodium cacodylate, pH 7.0; 23 °C.

Ultraviolet and derivative mixing curves show that (dA)$_n$ and (rT)$_n$ form only a 1:2 complex (Figure 6; Figure 4S in supplementary material). (rA)$_n$ and (rT)$_n$ have been shown to form both 1:1 and 1:2 complexes (Howard et al., 1971). Exclusively 1:1 stoichiometry has been established for (rA)$_n$ and (dT)$_n$ in 0.1 M Na^+ (Riley et al., 1966), though some evidence suggested a 1:2 complex was formed in 3.8 M Na^+. Infrared spectra of a 1:2 mixture in 3.7 M Na^+, however, show only bands characteristic of the double helix (Figure 5S in supplementary material).

Infrared spectra can also be used to establish stoichiometry of AU helices (Miles & Frazier, 1964; Howard et al., 1971, 1976). An explicit infrared study of the helices in Table I will be reported separately. We use this method here to establish that (d2NH$_2$A)$_n$·(rT)$_n$ undergoes a 2→3 transition on heating. The infrared spectrum of this complex resembles other two-stranded A·T complexes (cf. references above) in having two carbonyl bands at ~1686 and 1675 cm^{-1} and a T ring vi-

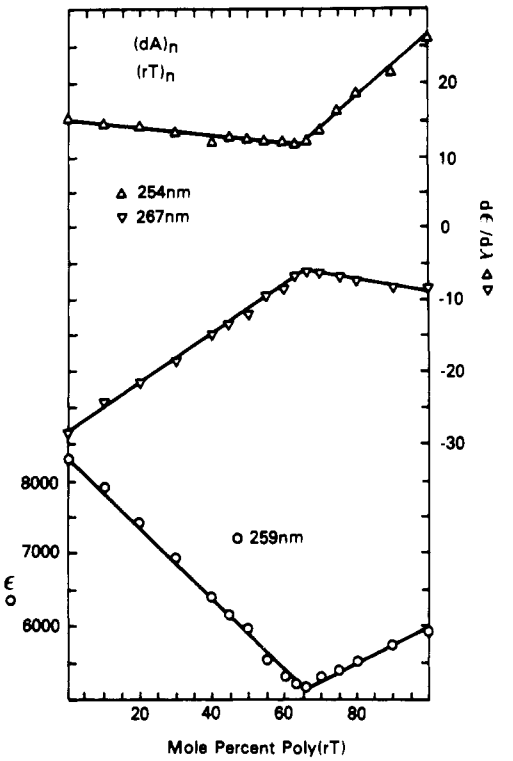

FIGURE 6: Single break at the 1:2 ratio in both ultraviolet [(O) left scale] and derivative ultraviolet [(△, ▽) right scale] mixing curves at three different wavelengths demonstrate formation of poly(dA)·2poly(rT). Conditions: 6×10^{-5} M total polymer P; 0.002 M sodium cacodylate, pH 7.0; 0.1 M Na^+; T = 20.0 °C.

bration at 1635 cm^{-1}. Heating to 70 °C causes frequency shifts and intensity reductions in the carbonyl region, and three new bands appear at 1692, ~1680 (sh), and 1659 cm^{-1}. The T and A ring vibrations are at ~1635 and 1614 cm^{-1}, respectively. This spectrum, which closely resembles that of the A·2T triple helix (Howard et at., 1971), persists until temperatures above ~80 °C are reached and then melts sharply to that of the single strands (Figure 6S in supplementary material). The first step of the biphasic melting curve is therefore a disproportionation: $2(d2NH_2A)_n{\cdot}(rT)_n \rightarrow (d2NH_2A)_n{\cdot}2(rT)_n + (d2NH_2A)_n$. The second is a 3 → 1 transition: $(d2NH_2A)_n{\cdot}2(rT)_n \rightarrow (d2NH_2A)_n + 2(rT)_n$.

Circular Dichroism. The CD spectra of the four homopolymer complexes of 2NH$_2$A and T are shown in Figure 7 and Table I. Three of the four spectra have negative first extrema, and the first two bands are conservative in all cases. Assignments and structural interpretations are presented under Discussion.

Thermal Transitions. $(d2NH_2A)_n{\cdot}(dT)_n$ melts sharply (σ = 3°; breadths of all thermal transitions are given in Table IIS in supplementary material) in a 2 → 1 transition with T_m = 77 °C in 0.1 M Na^+ (Howard & Miles, 1983a). The slope of the salt dependence curve for the 3 → 2 transition is unusually high (42.6°). The phase diagram is shown in Figure 8.

The interaction of $(d2NH_2A)_n$ with $(rT)_n$ is much more complex than with $(dT)_n$ and in a number of ways resembles the $(rA)_n$,$(rU)_n$ system (Miles & Frazier, 1964; Stevens & Felsenfeld, 1964; Krakauer & Sturtevant, 1968). The phase diagram (Figure 9) shows a 2 → 1 transition only below 0.04 M Na^+ and a 3 → 2 transition in the same range of ionic strength. The double helix undergoes a disproportionation (2 → 3) above 0.1 M Na^+ (cf. section on IR spectra) and the triple helix a 3 → 1 transition above 0.05 M Na^+. Phase diagrams for the systems $(r2NH_2A)_n$, $(rT)_n$ and

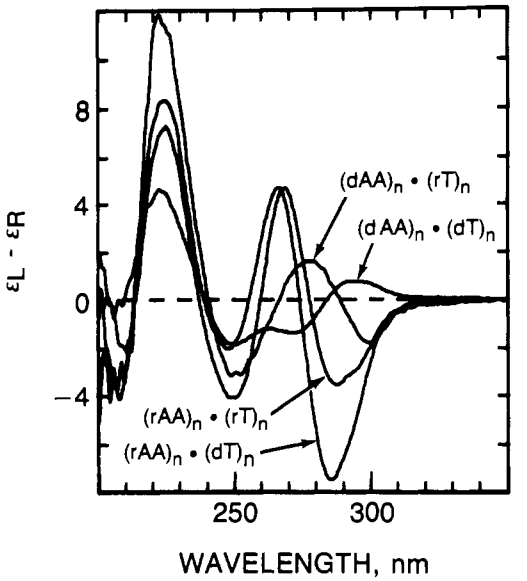

FIGURE 7: CD spectra of poly(d2NH$_2$A)·poly(dT), poly(d2NH$_2$A)·poly(rT), poly(r2NH$_2$A)·poly(dT), and poly(r2NH$_2$A)·poly(rT). Each spectrum is the average of nine runs and has been smoothed, base line corrected, and plotted by a computer. The spectrum of poly(d2NH$_2$A)·poly(dT) was measured at 5 °C and the others at 20 °C. AA ≡ 2NH$_2$A.

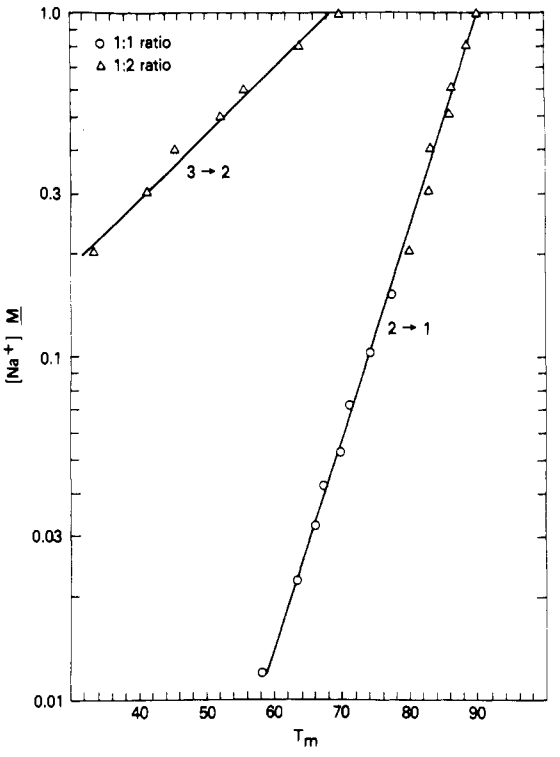

FIGURE 8: Phase diagram for the complexes poly(d2NH$_2$A)·poly(dT) and poly(d2NH$_2$A)·2poly(dT). The curve on the left relates T_m to [Na^+] for the 3 → 2 transition and on the right to the 2 → 1 transition. Estimates of dT_m/d log [Na^+] are listed in Table II.

$(r2NH_2A)_n$,$(dT)_n$ are given in Figure 7S (supplementary material) and those of $(rA)_n$,$(rT)_n$, $(dA)_n$,$(rT)_n$ and $(rA)_n$,$(dT)_n$ systems in Figure 8S and 9S (supplementary material). Data from 2NH$_2$A,T systems are summarized in Tables II and III, together with information on related systems. Our interpretations of the data are given under Discussion.

Discussion

The CD spectrum of $(d2NH_2A)_n$ (Table I) is quite similar to that of $(r2NH_2A)_n$, reported previously (Howard et al.,

Table II: Thermal Properties of Helices

	T_m/[Na$^+$]^a 0.03 M	0.1 M	dT_m/d log [Na$^+$]	$\Delta H°$ calcd kcal^{-1} bp^{-1}
a) $(r2NH_2A)_n$·$(rT)_n$	93	(100)	12.8 ± 0.7	13.8
b) $(rA)_n$·$(rT)_n$	62	73 (3/1)	18.3 ± 1.1	8.1
c) $(d2NH_2A)_n$·$(dT)_n$	66	77	16.4 ± 0.3	9.2
d) $(dA)_n$·$(dT)_n$	56	67	17.1 ± 0.6	8.4
e) $(r2NH_2A)_n$·$(dTe)_n$	84	91	12.9 ± 0.5	13.0
f) $(rA)_n$·$(dT)_n$	54	64	17.5	8.1
g) $(d2NH_2A)_n$·$(rT)_n$	71	81 (3/1)	14.7 ± 1.0	10.6
h) $(dA)_n$·$2(rT)_n$	48 (3/1)	62 (3/1)		
i) $(d2NH_2A\text{-}dT)_n$	70	76	13.3 ± 0.5	11.7
j) $(dA\text{-}dT)_n$	50	61		
k) $(d2NH_2A\text{-}dC)_n$·$(dG\text{-}dT)_n$	88	95	14.3 ± 0.3	12.0
l) $(dA\text{-}dC)_n$·$(dG\text{-}dT)_n$	81	89	16.2 ± 0.4	10.2
m) $(dA\text{-}dC)_n$·$(dI\text{-}dT)_n$	49	56.5	15.1 ± 0.3	9.0
n) $(d2NH_2A\text{-}dC)_n$·$(dI\text{-}dT)_n$	57	66	14.3 ± 0.7	10.1

^{a} T_m in 0.03 M Na$^+$ refers to a 2 → 1 transition in all cases except (h). T_m in 0.1 M Na$^+$ refers to a 2 → 1 transition unless otherwise noted and to a 3 → 1 transition when followed by the notation (3/1). Values in parentheses are extrapolated. Values for (a–e), (g–i), and (k–n), this work; from (f) Riley et al. (1966). For the helices studied in this report, T_m at any salt concentration in the stated ranges may be determined from the equations of Table III within the standard error stated there.

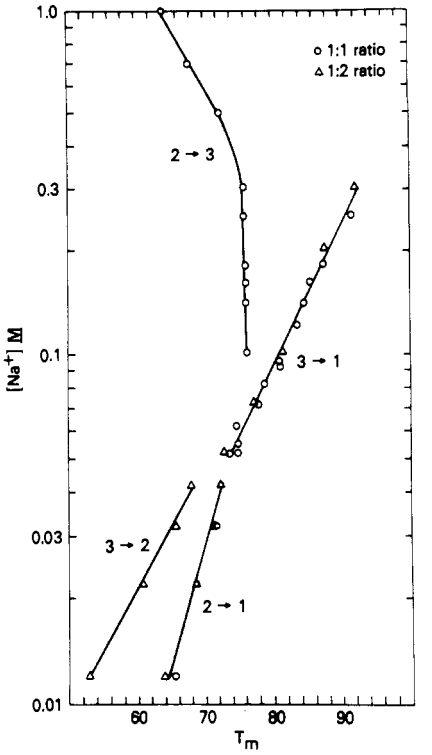

FIGURE 9: Dependence of T_m upon [Na$^+$] for four transitions of the poly(d2NH$_2$A), poly(rT) system. Estimations of dT_m/d log [Na$^+$] for linear curves are listed in Table II.

1976). In the UV spectrum, the B_{1u} and B_{2u} transitions of $(d2NH_2A)_n$ are clearly resolved at 257 and 279 nm, respectively (Figure 1), and the four CD extrema in this region (292, 272, 257, and 247 nm) are assigned to exciton splitting of these transitions (cf. Howard et al., 1976; Howard & Miles, 1983b). The bands at 222 and 207 nm presumably result from splitting of the E_{1u} transition at 214 nm.

CD spectra of the four homopolymer duplexes (Figure 7) show marked differences, which are, nevertheless, consistent with a common structural and spectroscopic interpretation. The long wavelength extrema (286–298 nm) are assigned in all cases to exciton splitting of the B_{2u} transition of $2NH_2A$. The first two bands are conservative in all cases, with crossovers occurring near the mean of the wavelengths of these bands. The second lobe of splitting of the B_{2u} transition contributes to the second extremum (269–275 nm), as does, presumably, the B_{2u} transition of T. The B_{1u} transition of $2NH_2A$ produces only weak CD bands in $(d2NH_2A)_n$ and $(r2NH_2A)_n$ and appears to do so as well in spectra of these four helices. We suggest that the two bands at ~224 and ~205 nm result from splitting of the $2NH_2A$ transition at ~214 nm [for reasons supporting these assignments, cf. Howard et al. (1976) and Mathelier et al. (1979)].

The most unusual aspects of the spectra of Figure 7 are the sign reversal of the first pair of bands of $(d2NH_2A)_n$·$(dT)_n$ with respect to the other three spectra and the negative sign of the longest wavelength extremum in three cases. A similar negative band is observed at 286 nm in $(r2NH_2A)_n$·$(rU)_n$ (Howard et al., 1976). In all examples with a negative first band the composition of the complex is either ribo–ribo or hybrid. While DNA can have the A and B, as well as other conformations, both natural and synthetic RNA regular helices have been reported in the A or A′ form. Ribo–deoxy hybrids generally have been believed to be the A form [cf. Milman et al. (1967), Arnott (1970), and O'Brien & MacEwan (1970)]. Wang et al. (1982) have recently reported that a ribo–deoxy hybrid oligomer exists in the A form both in the crystal and in solution. Zimmerman & Phieffer (1981), on the other hand, have found that $(rA)_n$·$(dT)_n$ has diffraction patterns at high humidity similar to those of B-DNA. In their proposed model conformation of the rA strand resembles those in models of A-RNA or A-DNA, with similar dihedral angles

Table III: Dependence of T_m on log [Na$^+$]

	transition	range of [Na+]	no. of observations	SE of estimate, $\sigma_{x,y}$	equation
$(d2NH_2A)$·$(dT)_n$	2 → 1	0.01–1.0	15	0.7510	T_m = 16.408 log [Na$^+$] + 90.26
$(d2NH_2A)$·$2(dT)_n$	3 → 1	0.2–1.0	7	1.442	T_m = 52.442 log [Na$^+$] + 68.44
$(d2NH_2A)$·$(rR)_n$	2 → 1	0.01–0.04	8	0.5717	T_m = 14.694 log [Na$^+$] + 92.94
$(d2NH_2A)$·$2(rT)_n$	3 → 1	0.05–0.3	19	0.6704	T_m = 24.607 log [Na$^+$] + 105.4
$(d2NH_2A)$·$2(rT)_n$	3 → 2	0.01–0.04	4	0.4996	T_m = 61.750 log [Na$^+$] + 106.9
$(r2NH_2A)$·$(dT)_n$	2 → 1	0.01–0.14	13	0.4943	T_m = 12.834 log [Na$^+$] + 103.8
$(r2NH_2A)$·$(rT)_n$	2 → 1	0.02–0.03	5	0.1281	T_m = 12.803 log [Na$^+$] + 111.9
$(r2NH_2A)$·$2(rT)_n$	3 → 2	0.02–0.03	3	0.0494	T_m = 25.350 log [Na$^+$] + 83.01
$(dA)_n$·$(dT_n$	2 → 1	0.05–0.3	5	0.4170	T_m = 17.045 log [Na$^+$] + 81.68
$(dA)_n$·$2(rT)_n$	3 → 1	0.01–0.5	10	0.5045	T_m = 25.850 log [Na$^+$] + 87.81
$(rA)_n$·$(dT)_n$	2 → 1	0.07–0.3	4	0.6578	T_m = 14.729 log [Na$^+$] + 78.68
$(rA)_n$·$(rT)_n$	2 → 1	0.01–0.03	4	0.4074	T_m = 18.257 log [Na$^+$] + 89.04
$(rA)_n$·$2(rT)_n$	3 → 1	0.05–0.7	18	0.3396	T_m = 22.609 log [Na$^+$] + 96.09
$(rA)_n$·$2(rT)_n$	3 → 2	0.01–0.03	3	0.4881	T_m = 35.904 log [Na$^+$] + 115.4

and C3-endo sugar pucker. The dihedral angles of the dT strand are not very similar to those in B-DNA, though the pucker is C3-exo. Despite these differences in backbone conformation, the helical parameters (pitch, axial rise, and residues per turn) at high humidity, and the X-ray diffraction pattern, are quite similar to those of B-DNA. A survey by Zimmerman & Pheiffer (1981) of several other hybrids under highly hydrated conditions, however, yielded no other clear examples of B-DNA-like diffraction patterns.

For the present we assign the ribo–deoxy hybrids in Table II to an A conformation, while recognizing that some of the deoxy strands may have backbone dihedral angles differing from typical A- or B-form values. The duplex with a positive first band at 297 nm is deoxy–deoxy and presumably has the B conformation at moderate ionic strength. We note that S-2L DNA, in which all A residues are replaced with $2NH_2A$, also has a positive first extremum at 290 nm (Kirnos et al., 1977). Three further synthetic DNAs with the $2NH_2A$ chromophore also have positive first extrema at 285–292 nm: $(d2NH_2A\text{-}dC)_n$·$(dG\text{-}dT)_n$, $(d2NH_2A\text{-}dC)_n$·$(dI\text{-}dT)_n$, and $(d2NH_2A\text{-}dT)_n$ (Howard & Miles, 1983b; Howard et al., 1984). It thus appears that the B_{2u} transition of $2NH_2A$ leads to a positive first extremum at ~290 nm in B-form helices and to a negative first band in A-form duplexes.

A significant finding of recent work with 2-aminoadenine is the marked difference in elevation of T_m between the ribo and deoxy series (cf. Howard & Miles, 1983a). We discuss the available data below and propose an explanation of this phenomenon later in this paper.

Data on the effects of $2NH_2$ substitution on T_m are summarized in Table II. Comparisons may be made between duplexes that have identical ribo–deoxy composition and that differ only in the presence or absence of a 2-NH_2 group in the purine residues. Conformational assignments are discussed in the preceding paragraphs. Significant regularities are observed in T_m differences for relevant pairs of helices in Table II. Thus, T_m elevations for the 2-NH_2 group in B-form helices are 10 (c – d), 15 (i – j), and 12 °C [2(k – l)]. For 2-aminoadenine in A-form helices in 0.1 M Na^+, the value is 27 (a – b and e – f). If we take 12 and 27 °C as representative values, the difference in T_m elevation between the A and B series is approximately 15 °C.

The difference in properties of G and I helices is obviously relevant to the difference for $2NH_2A$ and A, but satisfactory thermal data are much more difficult to obtain. Though full salt dependence curves are available for $(dG)_n$·$(dC)_n$ (Inman & Baldwin, 1964) and $(dG\text{-}dC)_n$ (Wells et al., 1970), very high transition temperatures have limited the data on $(dG)_n$·$(rC)_n$, $(rG)_n$·$(dC)_n$, and $(rG)_n$·$(rC)_n$ to a single T_m in 10^{-3} M Na^+ (Chamberlin, 1965). In addition to problems posed by inaccessible temperatures, the transitions of the homopolymer helices are not simple helix–coil transitions. Infrared studies indicate that the form of $(rG)_n$ after dissociation of $(rG)_n$·$(rC)_n$ (~0.01 M) is not single stranded but rather an ordered form of the polymer (Miles & Frazier, 1982). Coupled G and C carbonyl bands (1688, 1647 cm^{-1}) characteristic of the G·C pair (Howard et al., 1969) do not reappear when the solution is cooled. Similar results are observed when $(dG)_n$·$(dC)_n$ (0.005 M in polymer phosphate) is melted and recooled. Nevertheless, we may obtain a qualitative indication of the G – I difference by making the arbitrary assumption that $dT_m/d \log [Na^+] = 18$ °C for the presumably A-form G·C helices. The estimates for T_m elevation by 2-NH_2 of G are then 73 °C for $[(rG)_n$·$(rC)_n - (rI)_n(rC)_n]$, 74 °C for $[(rG)_n$·$(dC)_n - (rI)_n$·$(dC)_n]$, and 72 °C for $[(dG)_n$·$(rC)_n - (dI)_n$·$(rC)_n]$. For the deoxy–deoxy (and presumably B-form) helices measured values can be used. The ΔT_m values are 54 °C for $[(dG)_n$·$(dC)_n - (dI)_n$·$(dC)_n]$, 56 °C for $[(dG\text{-}dC)_n - (dI\text{-}dC)_n]$, 58 °C for $[(d2NH_2A\text{-}dC)_n$·$(dG\text{-}dT)_n - (d2NH_2A\text{-}dC)_n$·$(dI\text{-}dT)_n]$, and 65 °C for [(dA-dC)·(dG-dT) – (dA-dC)·(dI-dT)]. [The following are the sources of GC data cited above: IC homopolymer data from Chamberlin & Patterson (1965); $(dI\text{-}dC)_n$ data from Wells et al. (1970); data on systems derived from (AC)·(GT), this study.] The difference in T_m between GC and IC helices would be roughly 15 °C greater in the ribo than in the deoxy series on the basis of the above discussion. For reasons stated above this value is uncertain, though it is probably adequate to indicate qualitative agreement with the $2NH_2A$ – A difference and with the subsequent discussion. We should note that reasons for larger T_m elevations in (G·C)-(I·C) pairs than in $(2NH_2A$·T)-(A·T) pairs are not addressed in this report. We assume they are related to different stacking interactions. The important point for the present study is that this aspect of the interaction can be factored out by the above approach, permitting a comparison of hydrogen-bonding effects in the two series.

Formation of a third hydrogen bond in A·T and A·U pairs appears to be the primary factor responsible for T_m elevation by $2NH_2A$ in ribopolynucleotide helices. In related studies, amino groups have been introduced into the 2-position of adenosine monomers which form helices with complementary polymers and into the 8-position of both A and G monomers and polymers having geometry favorable for hydrogen bonding of the introduced amino group (Howard et al., 1966, 1976; Ikeda et al., 1970; Hattori et al., 1975, 1976). In all cases there has been a marked elevation of T_m whether the amino group is introduced into A or G, into the 2- or the 8-position. When more than one complex is possible, the one actually formed is that having the larger number of hydrogen bonds [see, for example, discussion in Hattori et al. (1975, 1976) and Howard et al. (1976)]. If additional hydrogen bonds have such effects in the ribopolynucleotide series, why are the T_m elevations significantly smaller with both $2NH_2A$·T and G·C deoxypolynucleotide helices? The effect of hydrogen bonding would be expected to be similar in both ribo and deoxy series. We suggest an explanation may be found in recent crystallographic studies from Dickerson's laboratory (Dickerson et al., 1982; Drew & Dickerson, 1981). In the B-form dodecamer, CGCGAATTCGCG, many ordered water molecules were located, and a specific two-layer spine of hydration was identified in the minor groove. This pattern exists only in the AATT region of the helix (and only in B-form DNA) and is disrupted by the 2-NH_2 group of G. Dickerson et al. (1982) suggest that this hydration pattern makes a large contribution to stabilizing the B-form helix and that 2-aminoadenine would, like G, disrupt this pattern, presumably with a reduction of stability in the B-form helix. We suggest that the observed effect of $2NH_2A$ substitution and of the same 2-NH_2 difference between I and G in the deoxypolynucleotide series result from two opposing effects: (a) stabilization by introduction of a third hydrogen bond, as in the series cited above, and (b) destabilization by disruption of the spine of hydration of B-form helices. The differential in T_m elevation by the 2-NH_2 group in the ribo and deoxy series suggests that the spine of hydration contributions roughly 15 °C in T_m to stabilizing B-form helices in which it is present.

A further measure of the contribution of $2NH_2A$ to the energetics of helix formation can be derived from slopes of the salt dependence curves of the different complexes (cf. Figures 8 and 9 and 7S and 8S of supplementary material; Table II).

Table IV: Observed and Calculated Enthalpies

substance	T_m[a] (°C)	dT_m/d log [Na^+]	ΔH° (exptl)	ΔH° (calcd)
poly(rI)·poly(rC)	80.7	17.6	8.86[b]	9.30
poly(rI)·poly(rBrC)	80.7	17.5	9.67[c]	9.36
T2 phage DNA	80.7	19.2	9.47[d]	8.53
poly(dA)·poly(dT)	56	17.1	8.60[e]	8.29

[a] Comparisons of ΔH (exptl) and ΔH (calcd) are made at elevated T_m values, where possible, to minimize energetic contributions of single-strand stacking interactions. [b] Extrapolated value from the data of Hinz et al. (1970). [c] Extrapolated value from the data of Ross et al. (1971). [d] Interpolated value from the data of Privalov et al. (1969). [e] Data of Marky & Breslauer (1982).

The slopes dT_m/d log [Na^+] in the ribo series are consistently lower when r2NH_2A rather than rA is present, and the slopes for r2NH_2A systems are lower than for the deoxy systems, whether d2NH_2A or dA is present.

Manning has applied his polyelectrolyte theory to the denaturation of DNA and obtained a relationship between ΔH and dT_m/d log [Na^+] (1972, 1978, and references cited therein). We apply this relationship in the form employed by Record et al. (1978) to calculate ΔH of melting from our observed slopes. In support of this application, we show below that it reproduces available observed calorimetric values with reasonable accuracy (Table IV).

The equation employed (Record et al., 1978) is

$$\frac{dT_m}{d \ln a_\pm} = \alpha \frac{RT_m^2}{\Delta H^\circ_{obsd}} \frac{\Delta\bar{\theta}_{M^+}}{2}$$

where ΔH°_{obsd} is the observed enthalpy of transition per mole of nucleotides, $a_\pm$ = mean activity and is assumed $\simeq a$, α = $[1 + d \ln \gamma_\pm / d \ln a_\pm] \approx 0.95$ for $10^{-3} M \leq [Na^+] \leq 10^{-1}$ M, $\gamma_\pm$ = mean activity coefficient, and $\Delta\bar{\theta}_{M^+}$ = the number of counterions released per phosphate denatured.

We use the value of $\Delta\bar{\theta}_{M^+} = 0.32$, from Record et al. (1978), who obtained it by using ΔH° for AU → A + U reported by Krakauer & Sturtevant (1968). The calculated and observed values for three synthetic polynucleotide helices and T2 DNA in Table IV agree with an average deviation of ±5%. ΔH° values calculated for helices relevant to the present study are given in Table II.

Many factors contribute to the observed enthalpy of melting of a helix, most of them not ascertainable from the net value. By determination of differential values of pairs selected for the presence and absence of specific features, however, it is possible to isolate some of the component factors and estimate their magnitudes. Taking the difference in ΔH for the pair a – b in Table II, for example, we obtain a $\Delta(\Delta H)$ value of –5.7. The ribo–deoxy composition is the same within each pair, the conformation is presumably A form (see above) with no spine of hydration, and we assume that the contribution of base stacking, for example, is approximately the same within each pair. We therefore take a value of roughly –5 kcal to represent primarily a stabilizing enthalpic contribution of the 2-amino group for the A conformation. For the deoxy pair c – d, however, $\Delta(\Delta H)$ is only –0.8 kcal. In this case, both helices are presumably B form, d with a spine of hydration and c without. For the pair n – m, the difference 2 × 1.1 = 2.2 kcal is obtained. We suggest that the 2-NH_2 group contributes two effects acting in opposite directions: it stabilizes the B-form helix by an additional interbase hydrogen bond and simultaneously destabilizes it by disrupting the spine of hydration.

It may be seen from Table II that there is little difference in ΔH of transition between ribo- and deoxypolynucleotide (or A and B form) helices which lack the 2-NH_2 substituent. Thus, the pair b – d, for example, has a $\Delta(\Delta H)$ value of –0.3 kcal. This rough equality of ΔH in A- and B-form helices appears to depend upon the presence of the spine of hydration in the B form. When this bilayer is excluded by a 2-NH_2 group, as in the pair a – c, a large difference of 3–4 kcal is found.

The importance to helix stability of hydration at a specific site was shown in an earlier study of interaction between $(r2NH_2A)_n$ and $(rI)_n$ (Howard et al., 1977). Though both $(rA)_n$ and $(r2MeA)_n$ form exclusively triple helices with $(rI)_n$, $(r2NH_2A)_n$ was found to form only a double helix, with base pairing of I to the N7 position of $2NH_2A$ and none at N1. While an I residue in the usual Watson–Crick position would have no electronegative atom to hydrogen bond to the nearer 2-NH proton of $2NH_2A$, the hypoxanthine base would block a water molecule from occupying a position in which it could form a bond to the 2-NH proton. This indirect solvation effect, mediated by the energetics of the helix–coil equilibrium, is sufficient to prevent pairing that would otherwise occur on the N1 side of $2NH_2A$ (Howard et al., 1977). The hydration effect with $2NH_2A$·I is much larger than that of the spine of hydration in DNA since, in the latter case, other H-bonding solvent arrangements, though presumably less regular and less favorable, can exist after the water bilayer is disrupted.

Phase diagrams of the homopolymer systems reported here exhibit remarkable diversity (Figures 8 and 9 and 7S and 8S in supplementary material). Though the two homologous systems $(d2NH_2A)_n$,$(dT)_n$ and $(r2NH_2A)_n$,$(rT)_n$ have the same transitions, the much lower stability of the triple helix in the former, reflected by low $T_{m(3\rightarrow2)}$ and high slope of the 3 → 2 transition curve, is apparent. The large elevation of $T_{m(2\rightarrow1)}$ for 2-NH_2 substitution in the ribo series contrasted with a small elevation in the deoxy series has been discussed above. A 2 → 3 transition does not occur in either of these systems. The two ribo–deoxy hybrids resemble the ribo pair in having large T_m elevations for the 2-NH_2 group. These hybrid systems, $(d2NH_2A)_n$,$(rT)_n$ and $(r2NH_2A)_n$,$(dT)_n$ (Figure 9; Figure 7S in supplementary material), however, exhibit a large and surprising difference from each other as well as from the two homologous systems. $(r2NH_2A)_n$·$(dT)_n$ forms no triple helix under any of the conditions examined ([Na^+], 0.01–1.0 M; Figure 2 and Figure 3S in supplementary material). The second hybrid, $(d2NH_2A)_n$·$(rT)_n$, in marked contrast, shows a highly stable triple helix [$T_{m(3\rightarrow2)}$ = 67 °C in 0.04 M Na^+; Figure 4]. A thermal conversion of double to triple helix (2 → 3) occurs at all salt concentrations above 0.07 M. The general form of the phase diagram (Figure 9) is quite similar to that of $(rA)_n$,$(rT)_n$ (Figure 8S in supplementary material). Separation of the second rT strand of the triple helix (which does not participate in 2-NH_2 hydrogen bonding) in the 3 → 2 transition occurs at essentially the same temperature in both systems.

We observe significant differences in T_m for the 2 → 1 (or 3 → 1) transition in the ribo and deoxy series, analogous to those reported by Riley et al. (1966) and Chamberlin & Patterson (1965). The sequence, however, is different: $(r2NH_2A)_n$·$(rT)_n$ > $(r2NH_2A)_n$·$(dT)_n$ > $(d2NH_2A)_n$·$(rT)_n$ > $(d2NH_2A)_n$·$(dT)_n$. We have added pairs containing rT to the series reported by Riley et al. (1966) to complete the sequence: $(rA)_n$·$(rT)_n$ > $(dA)_n$·$(dT)_n$ > $(rA)_n$·$(dT)_n$ > $(dA)_n$·$2(rT)_n$. For the former series, the difference between the first and last member is 24 °C in 0.1 M Na^+ [cf. 25 °C for the IC series (Chamberlin & Patterson, 1965)] and for the latter 18 °C. In view of the differences between A- and B-form geometry and variations within the B family (cf. Dickerson et al., 1982), it appears that T_m differences of this magnitude could be

accounted for by conformational differences in the helices, though specific hydration patterns may also contribute.

The greatest difference among these systems, and the one largely responsible for the wide divergence in patterns of the phase diagrams, is in the stability of the triple helices. We note that addition of a second T strand to a double helix does not directly involve the 2-NH_2 group and that a similar pattern is observed with A·T and with 2NH_2A·T pairs.

Data on related phase diagrams, from this study and from the literature, may be summarized by placing interacting AT systems in four categories:

(A) The first category includes those systems which have only a double helix and a 2 → 1 transition in the usual range of observation [(r2NH_2A)$_n$·(dT)$_n$, (rA)$_n$·(dT)$_n$] (e.g., Figure 9S in supplementary material).

(B) The second category includes those systems which have only a triple helix and a 3 → 1 transition [(dA)$_n$·(rT)$_n$] (Figure 9S in supplementary material).

(C) The third category includes those which form both double and triple helices but have only the 3 → 2 and 2 → 1 transitions [(r2NH_2A)$_n$·(rT)$_n$, (d2NH_2A)$_n$·(dT)$_n$, (dA)$_n$·(dT)$_n$] (Figures 8 and 8S in supplementary material).

(D) The fourth category includes those which form both double and triple helices and have four transitions: 2 → 1, 3 → 2, 2 → 3, 3 → 1 [(d2NH_2A)$_n$·(rT)$_n$, (rA)$_n$·(rT)$_n$] (Figures 9 and 8S in supplementary material).

In groups A and C, the triple helix is destabilized with respect to the double helix, and in (B) and (D), it is stabilized. We note that in groups A and C (third strand is relatively destablized or not observed), the pyrimidine component is, with one exception, deoxy, whereas the purine component is either ribo or deoxy. In groups B and D, on the other hand, the pyrimidine component is always ribo. Again the purine component is either ribo or deoxy.

We consider the 3 → 2 transition temperature to be the most direct measure of stability of the triple helix and select 0.03 M in Na^+ as an ionic strength at which different systems can be compared. The lowest T_m is −9 °C (extrapolated) for (d2NH_2A)$_n$·2(dT)$_n$, and the highest is 64 °C for (d2NH_2A)·2(rT)$_n$, a difference of 73 °C. A similar T_m of 61 °C is observed for (rA)$_n$·2(rT)$_n$. Here again rT is associated with very stable attachment of the third strand and dT with unstable attachment. The large T_m difference of ~70 °C, moreover, is much greater than differences observed for introduction of the 2-NH_2 group into A or for differences for $T_{m(2\rightarrow1)}$ between the ribo and deoxy ribo series (cf. Chamberlin & Patterson, 1965; Riley et al., 1966). The reason for this difference in stability of the third strand is not clear. It evidently cannot be attributed to self-structure of the dissociated pyrimidine strand, since (rT)$_n$ has a fairly stable helix while (dT)$_n$ has none. We may suggest the existence in the hybrid helices of subtle conformational differences, which may require either more or less favorable geometry in the third strand if it is to attach to available sites on the double helix. Related to this conformational hypothesis is the possibility of different patterns of hydration, which could affect the 2 → 3 balance either by direct stabilization (cf. the spine of hydration in B-DNA) or indirectly by a large entropy increase when specifically ordered water molecules are released. Hydrogen bonding of the 2′-OH may also promote greater stability of attachment of (rT)$_n$ than of (dT)$_n$, by direct bonding either to the purine strand or to specific hydration patterns.

Supplementary Material Available

Two tables and nine figures containing data as described in the text (11 pages). Ordering information is given on any current masthead page.

References

Arnott, S. (1970) *Prog. Biophys. Mol. Biol. 21*, 267–319.

Bollum, F. J. (1966) in *Procedures in Nucleic Acid Research* (Cantoni, G., & Davies, D., Eds.) Vol. 1, pp 284–295, Harper and Row, New York.

Cerami, A., Reich, E., Ward, D. C., & Goldberg, I. H. (1967) *Proc. Natl. Acad. Sci. U.S.A. 57*, 1036–1042.

Chamberlin, M. J. (1965) *Fed. Proc., Fed. Am. Soc. Exp. Biol. 24*, 1446–1457.

Chamberlin, M. J., & Patterson, D. L. (1965) *J. Mol. Biol. 12*, 410–428.

Dickerson, R. E., Drew, H. R., Conner, B. N., Wing, R. M., Fratini, A. V., & Kopka, M. L. (1982) *Science (Washington, D.C.) 216*, 475–485.

Drew, H. R., & Dickerson, R. E. (1981) *J. Mol. Biol. 151*, 535–556.

Hattori, M., Frazier, J., & Miles, H. T. (1975) *Biochemistry 14*, 5033–5045.

Hattori, M., Frazier, J., & Miles, H. T. (1976) *Biopolymers 15*, 523–531.

Hinz, H.-J., Haar, W., & Ackermann, T. (1970) *Biopolymers 9*, 923–936.

Howard, F. B., & Miles, H. T. (1983a) *Biopolymers 22*, 597–600.

Howard, F. B., & Miles, H. T. (1983b) in *Nucleic Acids: The Vectors of Life* (Pullman, B., & Jortner, J., Eds.) pp 511–520, Reidel Publishing Co., Dordrect.

Howard, F. B., Frazier, J., & Miles, H. T. (1966) *J. Biol. Chem. 241*, 4293–4295.

Howard, F. B., Frazier, J., & Miles, H. T. (1969) *Proc. Natl. Acad. Sci. U.S.A. 64*, 451–458.

Howard, F. B., Frazier, J., & Miles, H. T. (1971) *J. Biol. Chem. 246*, 7073–7083.

Howard, F. B., Frazier, J., & Miles, H. T. (1976) *Biochemistry 15*, 3783–3795.

Howard, F. B., Hattori, M., Frazier, F., & Miles, H. T. (1977) *Biochemistry 16*, 4637–4646.

Howard, F. B., Chen, C.-W., Cohen, J. S., & Miles, H. T. (1984) *Biochem. Biophys. Res. Commun. 118*, 848–853.

Ikeda, K., Frazier, J., & Miles, H. T. (1970) *J. Mol. Biol. 54*, 59–84.

Inman, R. B., & Baldwin, R. L. (1964) *J. Mol. Biol. 8*, 452–469.

Kirnos, M. D., Khudyakov, I. Y., Alexandrushkina, N. I., & Vanyushin, B. F. (1977) *Nature (London) 270*, 369–370.

Krakauer, H., & Sturtevant, J. M. (1968) *Biopolymers 6*, 491–512.

Maniatis, T., Fritsch, E. F., & Sambrook, J. (1982) *Molecular Cloning*, p 438, Cold Spring Harbor Laboratory, Cold Spring Harbor, NY.

Manning, G. S. (1972) *Biopolymers 11*, 937–949.

Manning, G. S. (1978) *Q. Rev. Biophys. 11*, 179–246.

Marky, L. A., & Breslauer, K. J. (1982) *Biopolymers 21*, 2185–2194.

Mathelier, H. D., Howard, F. B., & Miles, H. T. (1979) *Biopolymers 18*, 709–722.

Maxam, A. M., & Gilbert, W. (1980) *Methods Enzymol. 65*, 499–560.

Miles, H. T., & Frazier, F. B. (1964) *Biochem. Biophys. Res. Commun. 14*, 21–28.

Milman, G., Langridge, R., & Chamberlin, M. J. (1967) *Proc. Natl. Acad. Sci. U.S.A. 57*, 1804–1810.

Moffat, J., & Khorana, H. G. (1961) *J. Am. Chem. Soc. 83*, 649–658.

Muraoka, M., Miles, H. T., & Howard, F. B. (1980) *Biochemistry 19*, 2429–2439.
O'Brien, E. J., & MacEwan, A. W. (1970) *J. Mol. Biol. 48*, 243–261.
Powell, J. I., Fico, R., Jennings, W. H., O'Bryan, E. R., & Schultz, A. R. (1980) *Proc. IEEE Comput. Soc., Int. Conf., 21st*, 185–190.
Privalov, P. L., Ptitsyn, O. B., & Birshtein, T. M. (1969) *Biopolymers 8*, 559–571.
Record, M. T., Anderson, C. F., & Lohman, T. M. (1978) *Q. Rev. Biophys. 11*, 103–178.
Riley, M., Maling, B., & Chamberlin, M. J. (1966) *J. Mol. Biol. 20*, 359–389.
Ross, P. D., Scruggs, R. L., Howard, F. B., & Miles, H. T. (1971) *J. Mol. Biol. 61*, 727–733.
Stevens, C. L., & Felsenfeld, G. (1964) *Biopolymers 2*, 293–314.
Tener, G. M. (1961) *J. Am. Chem. Soc. 83*, 158–168.
Wang, A. H.-J., Satoshi, F., van Boom, J. H., van der Marel, G. H., van Boeckel, S. A. A., & Rich, A. (1982) *Nature (London) 299*, 601–604.
Wells, R. D., Larson, J. E., Grant, R. C., Shortle, B. E., & Cantor, C. R. (1970) *J. Mol. Biol. 54*, 465–497.
Willis, J. E., Krocker, W. D., & Hassell, A. M. (1980) *Prog. Clin. Enzymol.*, 272–277.
Yoshikawa, M., & Kato, T. (1969) *Bull. Chem. Soc. Jpn. 42*, 3505–3508.
Zimmerman, S. B., & Pheiffer, B. H. (1981) *Proc. Natl. Acad. Sci. U.S.A. 78*, 78–82.

Mapping of Subsites in the Combining Area of Monoclonal Anti-Galactan Immunoglobulin A J539†

Cornelis P. J. Glaudemans,* Pavol Kováč, and Kjeld Rasmussen

ABSTRACT: Monoclonal immunoglobulin A J539 binds β-(1→6)-D-galactopyranans. Measurement of the affinity of its Fab′ fragment for a series of galacto oligosaccharides—some of which carried deoxyfluoro groups—has made it possible to assign a binding mode of the polysaccharide that has the reducing end oriented from the heavy (H) chain toward the light (L) chain. In addition, the values obtained for the affinity constants of the immunoglobulin with these oligosaccharides, as well as the maximal values obtained for the intrinsic ligand-induced fluorescence, permit a deduction about the relative affinity of the protein's four subsites for each galactose residue of the tetrasaccharide fragment it can bind. If these subsites are labeled C, A, B, and D, going from the H-chain toward the L-chain across the face of the immunoglobulin combining area, then the order of decreasing affinity is A > B > C > D.

Although monoclonal immunoglobulins have been affinity labeled (Givol et al., 1971), no detailed information of the interaction of a homopolysaccharide and its monoclonal immunoglobulin is available to date. Monoclonal immunoglobulin A (IgA) J539 has as its homologous antigen a β-(1→6)-D-galactopyranan, a neutral homopolysaccharide whose interaction with the antibody has been studied [Glaudemans, 1975; Jolley et al., 1974; Manjula & Glaudemans, 1976; Feldmann et al. (1981) and references cited therein; Roy et al., 1981; Ekborg et al., 1983]. IgA J539 Fab′ has been crystallized, but Navia et al. (1979) have observed that the cavity associated with the hypervariable clusters on the frontal surface of J539 is spatially blocked by the constant region of a neighboring, symmetry-related, molecule in the crystal lattice and that, indeed, soaking of these crystals in a solution of 6-*O*-β-D-galactopyranosyl-D-galactose, or of the corresponding tetrasaccharide, did not cause significant changes indicative of binding. Thus, it becomes important to endeavor to map the combining area of this IgA by means other than X-ray diffraction studies.

In order to evaluate the importance of H bonding between ligand and antibody, we have previously synthesized a number of deoxyfluorogalactosides and have already reported on the binding studies of some of these (Ittah & Glaudemans, 1981). In this paper we report the binding affinities of a larger number of such derivatives, which permit a conclusion as to important details of the binding mode of the homologous polysaccharide to IgA J539.

Materials and Methods

Ligands. The preparation of methyl 2-deoxy-2-fluoro-β-D-galactopyranoside (**1**) (Ittah & Glaudemans, 1981), methyl 3-deoxy-3-fluoro-β-D-galactopyranoside (**2**) (Kováč & Glaudemans, 1983a), methyl 4-deoxy-4-fluoro-β-D-galactopyranoside (**3**) (Ittah & Glaudemans, 1981), and methyl 6-deoxy-6-fluoro-β-D-galactopyranoside (**4**) (Kováč & Glaudemans, 1983b) has already been reported. The preparation of methyl 6-*O*-(β-D-galactopyranosyl)-β-D-galactopyranoside (**7**) (Kováč et al., 1984), methyl 6-*O*-(3-deoxy-3-fluoro-β-D-galactopyranosyl)-β-D-galactopyranoside (**8**) (Kováč & Glaudemans, 1983c), methyl 6-*O*-(6-*O*-β-D-galactopyranosyl-β-D-galactopyranosyl)-β-D-galactopyranoside (**9**) (Kováč et al., 1984b), and methyl 6-*O*-[6-*O*-(3-deoxy-3-fluoro-β-D-galactopyranosyl)-β-D-galactopyranosyl]-β-D-galactopyranoside, (**10**) has also been reported (Kováč & Glaudemans, 1983c, 1985), or their reports are in press. The preparation of methyl 6-deoxy-β-D-galactopyranoside (**6**) was as follows: D-Fucose (2 g) was dissolved in pyridine (10 mL) and cooled in ice, and acetic anhydride (10 mL) was added over a period of 1.5 h. The solution was left to warm up to room temperature and left overnight. The reagents were evaporated at 65 °C under vacuum, and traces were removed by flash evaporation with toluene under vacuum (3 times). ^{13}C

† From the National Institute of Arthritis, Diabetes, and Digestive and Kidney Diseases, National Institutes of Health, Bethesda, Maryland 20205 (C.P.J.G. and P.K.), and the Chemistry Department, The Technical University of Denmark, DK-2800 Lyngby, Denmark (K.R.). *Received May 7, 1984.*